*Human Molecular Genetics, 2015, Vol. 24, No. 2* **492–505**
*doi:10.1093/hmg/ddu469*
*Advance Access published on September 11, 2014*

# Loss of nNOS inhibits compensatory muscle hypertrophy and exacerbates inflammation and eccentric contraction-induced damage in mdx mice

**Stanley C. Froehner[1], Sarah M. Reed[1], Kendra N. Anderson[1], Paul L. Huang[2] and Justin M. Percival[1,3,*]**

[1]Department of Physiology and Biophysics, University of Washington Medical School, Seattle, WA, USA, [2]Cardiovascular Research Center and Harvard Stem Cell Institute, Massachusetts General Hospital, Boston, MA, USA and [3]Department of Molecular and Cellular Pharmacology, University of Miami Miller School of Medicine, Miami, FL, USA

Received June 12, 2014; Revised August 11, 2014; Accepted September 9, 2014

**Approaches targeting nitric oxide (NO) signaling show promise as therapies for Duchenne and Becker muscular dystrophies. However, the mechanisms by which NO benefits dystrophin-deficient muscle remain unclear, but may involve nNOSβ, a newly discovered enzymatic source of NO in skeletal muscle. Here we investigate the impact of dystrophin deficiency on nNOSβ and use mdx mice engineered to lack nNOSμ and nNOSβ to discern how the loss of nNOS impacts dystrophic skeletal muscle pathology. In mdx muscle, nNOSβ was mislocalized and its association with the Golgi complex was reduced. nNOS depletion from mdx mice prevented compensatory skeletal muscle cell hypertrophy, decreased myofiber central nucleation and increased focal macrophage cell infiltration, indicating exacerbated dystrophic muscle damage. Reductions in muscle integrity in nNOS-null mdx mice were accompanied by decreases in specific force and increased susceptibility to eccentric contraction-induced muscle damage compared with mdx controls. Unexpectedly, muscle fatigue was unaffected by nNOS depletion, revealing a novel latent compensatory mechanism for the loss of nNOS in mdx mice. Together with previous studies, these data suggest that localization of both nNOSμ and nNOSβ is disrupted by dystrophin deficiency. They also indicate that nNOS has a more complex role as a modifier of dystrophic pathology and broader therapeutic potential than previously recognized. Importantly, these findings also suggest nNOSβ as a new drug target and provide a new conceptual framework for understanding nNOS signaling and the benefits of NO therapies in dystrophinopathies.**

## INTRODUCTION

Defective nitric oxide (NO) signaling is a common pathogenic feature of many neuromuscular diseases including Duchenne and Becker muscular dystrophies (DMD and BMD), which are progressive muscle wasting diseases caused by mutations in the dystrophin gene (1–6). Loss of dystrophin inhibits NO signaling by preventing normal expression and subsarcolemmal scaffolding of neuronal nitric oxide synthase mu (nNOSμ), which synthesizes NO in skeletal muscle (3,7). nNOSμ expression is nearly eliminated from human dystrophin-deficient muscle and averages ∼20% of wild-type levels in mdx mice (a mouse model for DMD) (8). Inhibition of nNOSμ signaling has deleterious consequences for dystrophin-deficient muscle including: the inhibition of muscle repair, excessive sympathetic vasoconstriction, focal ischemic muscle damage during contraction and poor endurance exercise performance (9–16). Decreased nNOSμ expression may also disrupt its less well-defined cytoplasmic roles such as the regulation of mitochondrial biogenesis, RyR1 calcium channel and phosphofructokinase activity (11,14,17,18). Thus, the restoration of nNOSμ and NO signaling represents an important therapeutic approach for mitigating dystrophin-deficient muscle dysfunction.

Therapeutic approaches that increase NO and its key effector cGMP provide significant benefit to the dystrophic muscles of mdx mice and BMD patients (13,19,20). Indeed, the most therapeutically

*To whom correspondence should be addressed at: Department of Molecular and Cellular Pharmacology (R-189), University of Miami Miller School of Medicine, PO Box 016189, Miami, FL 33101, USA. Tel: +1 3052437303; Email: j.percival@med.miami.edu

efficacious gene therapy for DMD employs a microdystrophin that restores nNOSμ function, thereby improving endurance exercise performance (12). Normalization of NO levels in mdx muscles by muscle-specific expression of a nNOSα transgene reduced macrophage infiltration, muscle cell breakdown and central nucleation (21). Similar reductions in muscle inflammation and damage were reported using NO donors alone or in combination with anti-inflammatory drugs as well as studies using drugs with dual NO donor and anti-inflammatory activities such as HCT1026 (13,22). HCT1026 increased the fraction of centrally nucleated muscle cells, interpreted as improved muscle regeneration and repair, and restored NO regulation of sympathetic vasoconstriction (23).

NO can reduce muscle pathology through cGMP-dependent and S-nitrosation mechanisms (13,24). Targeting NO–cGMP signaling avoids the shortcomings of NO donor or releasing drugs which include off-target posttranslational modifications and NO tolerance (19,20). Amplifying NO–cGMP signaling with phosphodiesterase 5 (PDE5) inhibitors provides therapeutic benefit to dystrophic human and murine skeletal muscle through anti-fibrotic and vasodilatory activities (5,9,20,25). mdx mice treated with PDE5 inhibitors exhibit enhanced local blood delivery to active muscles, reduced skeletal muscle damage and faster recovery of ambulatory activity after mild exercise (5,9,25). Importantly, PDE5 inhibitors reduce diaphragm muscle fibrosis and weakness (25). The benefits of PDE5 inhibition and increased cGMP are not due to restoration of mitochondrial localization, content or ATP synthesis (26). As observed in NO-based studies, the impact of PDE5 inhibition on central nucleation remains unclear (9,25). Increases in NO or cGMP can increase (improved muscle regeneration), decrease (reduced degeneration) or have no effect on central nucleation suggesting a more complex relationship between NO and muscle repair (9,21,22,25). Nonetheless, these studies strongly support NO-based therapies as an attractive and pharmacologically amenable treatment option for DMD and BMD.

To realize the therapeutic potential of NO–cGMP signaling-based therapies, it is necessary to understand the extent to which nNOS modulates dystrophic pathology and the functions of nNOS–NO in dystrophin-deficient skeletal muscle. Furthermore, critical functions of nNOS, such as the regulation of contraction-induced fatigue, remain to be elucidated in dystrophin-null muscle. To date, the benefits of increased NO have been mostly attributed to activation of the predominant nNOSμ pathway in muscle (27). However, this interpretation requires critical reevaluation due to the recent discovery of a second skeletal muscle-expressed nNOS splice variant called nNOSβ that associates with the Golgi complex and possibly the sarcolemma (28,29). Thus activation of nNOSβ pathways may provide an additional mechanism by which increases in NO ameliorate dystrophic pathology.

Indeed, in contrast to predictions from most NO therapy studies, elimination of residual nNOSμ protein expression from dystrophin-deficient muscles has no impact on muscle permeability, central nucleation, inflammation or eccentric contraction-induced injury (13,30–32). In fact, despite the majority of studies suggesting that nNOSμ does not play a role in skeletal muscle strength (specific force), at least in non-dystrophic muscle, the loss of nNOSμ may actually enhance mdx muscle strength (32). While this has been attributed to a loss of nNOSμ-nitrosative stress, it is also possible that a compensatory increase in nNOSβ activity occurred which increased strength. Unlike nNOSμ, nNOSβ appears to regulate skeletal muscle strength (14,28). Indeed, compensatory increases in nNOSβ occur in the original isoform-specific 'nNOS knockout' mouse line (33). Thus, nNOSβ may be a compensatory source of NO in dystrophin-deficient skeletal muscle. Furthermore, it is also important to note that while the impact of dystrophin deficiency on nNOSμ has been extensively studied, the impact on nNOSβ is unknown. Therefore, to fully understand the role of NO in dystrophin-deficient muscles, we will also need to understand the role of nNOSβ in dystrophinopathy pathogenesis.

In the present study, we set out to define the role of nNOS in dystrophic pathogenesis by investigating whether loss of dystrophin negatively impacts nNOSβ and by generating mdx mice lacking residual nNOSμ and nNOSβ activity. Use of nNOS-null mdx mice circumvented the unaddressed issue of nNOS splice variant functional overlap and allowed us to investigate the full extent by which nNOS modulates clinically relevant features of dystrophinopathy pathogenesis. Here we demonstrate that, like nNOSμ, nNOSβ is also mislocalized in dystrophin-deficient muscle. We also show that loss of all nNOS activity from dystrophin-null muscle inhibits compensatory muscle hypertrophy, decreases central nucleation and exacerbates focal inflammation, indicative of increased muscle damage. Loss of nNOS also exacerbated muscle weakness under both isometric and eccentric stimulation conditions, but surprisingly did not impact muscle fatigue. Together with reports from other groups, these data provide the first evidence of a role for nNOSβ in modulating the severity of dystrophic pathology and suggest nNOSβ as a novel drug target. Furthermore, these findings support the notion that nNOS has a greater role in pathogenesis and greater therapeutic potential in dystrophinopathies than previously recognized.

## RESULTS

### Loss of dystrophin inhibits nNOSβ localization and association with the Golgi

To better understand the impact of dystrophin deficiency on nNOS signaling, we investigated whether nNOSβ localization was disrupted in adult 8-week-old mdx gastrocnemius muscles (Fig. 1). Because dystrophin is necessary for normal subsarcolemmal Golgi localization and density; we hypothesized that Golgi-associated nNOSβ should also be mislocalized in mdx muscles (34). In wild-type muscles, nNOSβ targeted to the subsarcolemmal Golgi complex marked by *cis*-Golgi compartment marker GM130 as reported previously (Fig. 1A) (28,34). nNOSβ colocalized with GM130 throughout the cytoplasm and at myonuclear poles (Fig. 1A) (34). Loss of dystrophin disrupted the 'beads on a string' localization of both GM130 and Golgi-associated nNOSβ (Fig. 1B). Quantitative analysis revealed that dystrophin deficiency decreased subsarcolemmal Golgi-nNOSβ densities by 39% ($P < 0.001$); thus affirming our hypothesis (Fig. 1C).

Reductions in nNOSβ densities could be explained in part by the reduction in GM130 densities that occur in the absence of dystrophin (34). To investigate the possibility that decreased nNOSβ densities were due to reductions in Golgi densities, we investigated

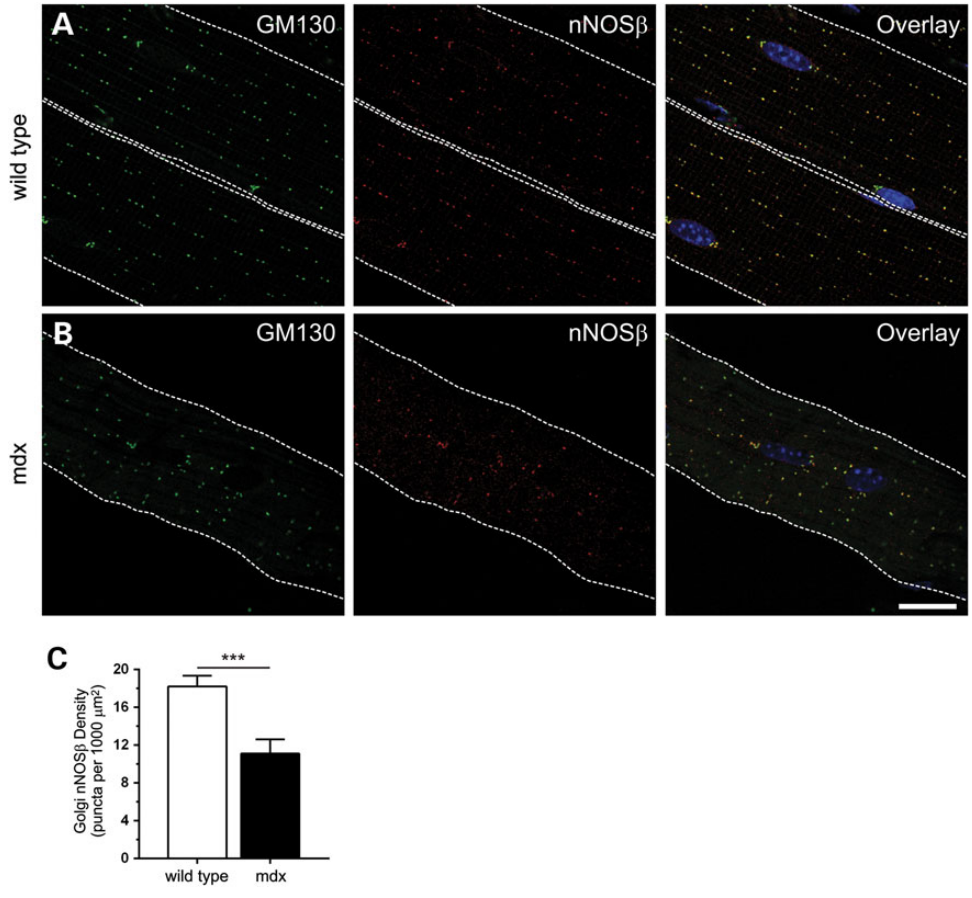


**Figure 1.** Loss of dystrophin causes mislocalization of Golgi-targeted nNOSβ. To determine the impact of dystrophin deficiency on nNOSβ localization, gastrocnemius myofibers from 8-week-old wild-type and mdx mice were immunolabeled with anti-GM130 and anti-nNOS antibodies. GM130 marks the *cis*-Golgi compartment. Nuclei (blue) were counterstained with DAPI. The sarcolemma is marked by a dashed white line. Single optical sections obtained by confocal microscopy are shown. (**A**) In wild-type muscle, nNOSβ exhibited stereotypic 'beads on a string' localization to the *cis*-Golgi compartment of the subsarcolemmal Golgi complex indicated by extensive colocalization with GM130. nNOSβ is also localized to the Golgi adjacent to myonuclei. (**B**) In mdx muscle, loss of dystrophin caused mislocalization of both the Golgi and nNOSβ. (**C**) Dystrophin deficiency caused a 39% reduction ($P < 0.001$) in subsarcolemmal Golgi-nNOSβ density (the number Golgi puncta positive for both GM130 and nNOSβ per 1000 $\mu m^2$) compared with wild-type controls. $^{***}P < 0.001$. $n = 6$ and 8 for wild-type and mdx groups, respectively. Scale bar: 20 microns.

Golgi-nNOSβ in 2-week-old mdx muscles which have the same subsarcolemmal GM130 localization and densities as wild-type muscle (34). Thus, a decrease in Golgi-nNOSβ density in 2-week-old muscles would indicate reduced targeting of nNOSβ to the *cis*-Golgi. As expected, nNOSβ-positive Golgi membranes were concentrated in an apparently stochastic distribution in the subsarcolemmal space and at myonuclei poles in 2-week-old wild-type myofibers (Fig. 2A). Also, Golgi-nNOSβ densities were lower in 2-week-old wild-type myofibers than in 8-week-old adult myofibers (compare Figs. 1C and 2C) reflecting developmental regulation of Golgi complex densities (34). Similar to wild-type controls, the Golgi complex was also stochastically distributed in 2-week-old mdx muscle cells (Fig. 2B). Note that a ~2-fold increase in the number of nuclei was also observed (not shown) compared with wild-type muscle which presumably reflects increased satellite cell fusion driving compensatory mdx muscle hypertrophy. However, a 42% reduction in Golgi-targeted nNOSβ was observed in 2-week-old mdx myofibers indicating that dystrophin deficiency impaired the association of nNOSβ with the Golgi complex (Fig. 2B and C). These data also suggest that impaired association of nNOSβ with the Golgi is not a secondary consequence of mdx muscle cell necrosis which begins at 3–4 weeks of age. It is important to note that while nNOS antibodies work well in immunofluorescence applications, they are not as reliable for detecting nNOSβ by western blotting in our hands. So we cannot test the possibility that the reduction in nNOSβ targeting to the Golgi in mdx myofibers is caused by decreased nNOSβ protein expression. Nonetheless, these data suggest that loss of dystrophin disrupts the spatial regulation of nNOSβ by promoting its mislocalization and inhibiting its association with the *cis*-membrane network of the subsarcolemmal Golgi complex.

### nNOS depletion prevents compensatory skeletal muscle hypertrophy in mdx mice

Given potential roles for NO in muscle growth and repair, we then investigated if loss of nNOS impacted muscle hypertrophy and damage in mdx mice (13,28,35,36). It is important to note that unlike dystrophin-deficient dogs or humans, mdx mice undergo compensatory muscle cell hypertrophy (37,38). The pathways responsible for this beneficial murine muscle growth

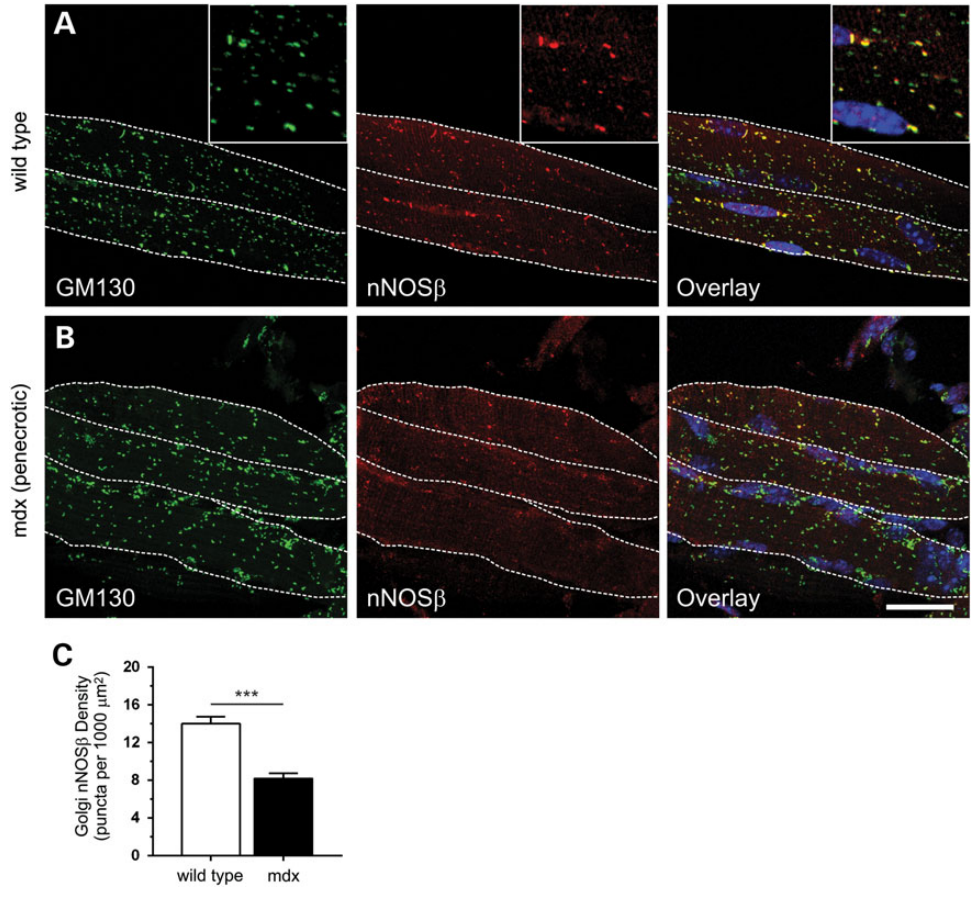


**Figure 2.** Reductions in Golgi-nNOSβ density in prenecrotic 2-week-old mdx muscle. To determine if nNOSβ association with the Golgi was decreased in mdx muscles, nNOSβ densities were determined in 2-week-old gastrocnemius myofibers from wild-type and mdx mice. Gastrocnemius myofibers were immunolabeled with anti-GM130 and anti-nNOS antibodies and nuclei counterstained with DAPI. Differences in myofiber geometry at 2 weeks necessitated the use of maximum projection images of myofibers which were obtained by confocal and two photon microscopy. The sarcolemma is marked by a dashed white line. (**A**) In 2-week-old wild-type muscle, the Golgi complex is non-uniformly distributed compared with adult muscle (left panel). But nNOSβ still colocalizes extensively with GM130 as in 8-week-old muscle. Yellow puncta in the overlay inset image highlight the high degree of association of nNOSβ with subsarcolemmal Golgi stacks, while green puncta represent intermyofibrillar Golgi stacks found deeper inside the muscle that lack nNOSβ. (**B**) In 2-week-old prenecrotic mdx muscle, loss of dystrophin has no impact on Golgi complex distribution relative to wild-type controls (left panel). However, prenecrotic muscles exhibit a marked reduction in Golgi-targeted nNOSβ (middle panel) highlighted in the overlay (right panel). (**C**) Dystrophin deficiency significantly reduced subsarcolemmal Golgi-nNOSβ density by 42% compared with wild-type controls. $^{***}P < 0.001$. $n = 5$ for wild-type and mdx groups. Inset image is 2.25× magnification. Scale bar: 20 microns.

are unclear, but represent potential clinical targets for reducing muscle wasting in DMD patients.

Because muscle size is proportional to body mass, we first investigated body mass. As expected, mdx mice exhibited normal body size; however, the body mass of nNOS-null mdx, now referred to as double knockout or DKO mice, was reduced by 20%, consistent with previous findings that nNOS is required for normal growth (Fig. 3A) (28,39). Glycolytic tibialis anterior (TA) muscles from mdx mice showed an expected 50% increase in mass that was inhibited by nNOS deficiency in DKO mice (Fig. 3B). Indeed, DKO TA masses were similar to wild-type controls. Oxidative soleus muscles were similarly affected in mdx and DKO mice (Fig. 3C). Thus nNOS is necessary for the compensatory hypertrophy of both glycolytic and oxidative muscles in mdx mice. Importantly, given previous reports that loss of nNOSμ has no impact on mdx muscle hypertrophy, our data suggest a role for nNOSβ in the compensatory muscle growth in mdx mice (30–32). To test if decreases in DKO muscle mass were the result of decreased body mass, TA and soleus muscle wet weights were normalized to body mass. Normalized mdx TA muscle masses were 53% greater than wild-type controls (Fig. 3D). Depletion of nNOS from mdx muscles substantially attenuated the increase in normalized TA muscle mass from 53 to 12% relative to wild-type controls. Loss of nNOS also prevented the increase in normalized soleus mass in DKO mice (Fig. 3E). Thus, reductions in muscle mass in DKO mice are likely due to both decreases in body mass and other mechanisms that remain to be defined.

To ascertain whether muscle mass reductions resulted from impaired muscle cell growth, the Feret diameters of individual myofibers were determined. In accordance with expected hypertrophy, mean mdx muscle cell Feret diameters were significantly larger than wild-type controls, whereas nNOS depletion decreased mean Feret diameter in DKO mice (mean Feret diameters: WT, 71 ± 2 μm; mdx, 93 ± 5 μm; DKO; 55 ± 5 μm) (Fig. 3F). Increased mdx myofiber size relative to wild-type was also indicated by an increased median Feret diameter and upward box shift in box and whisker plots reflecting a greater

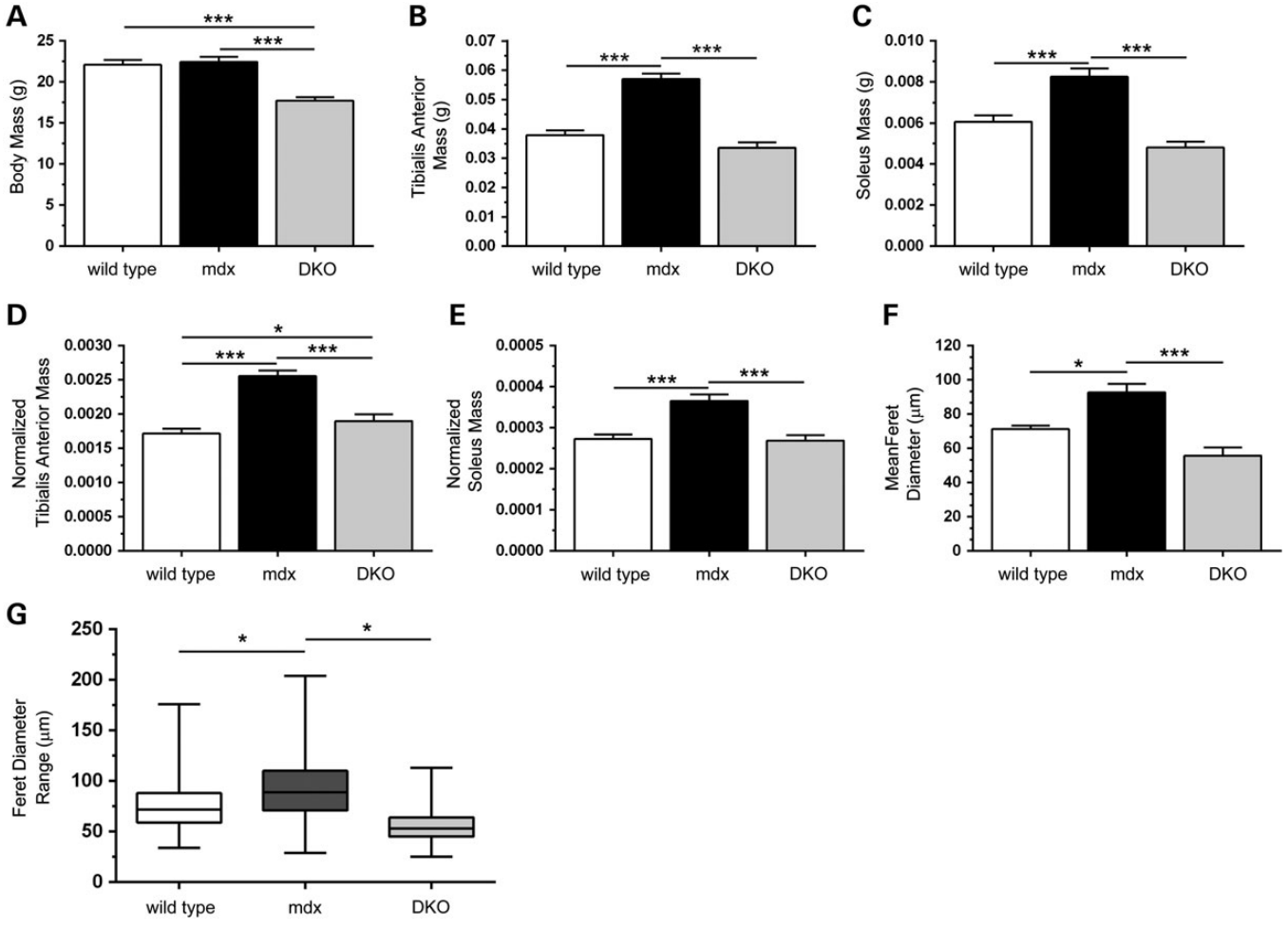


**Figure 3.** nNOSβ and nNOSμ depletion prevents compensatory skeletal muscle hypertrophy in mdx mice. (**A**) mdx mice lacking nNOSμ and nNOSβ (DKO) had decreased body mass compared with wild-type and mdx controls. (**B** and **C**) mdx mice exhibited a stereotypical increase in tibialis anterior (TA) and soleus muscle mass that was prevented by loss of nNOS. (**D** and **E**) Normalization of TA and soleus mass to body mass revealed that reductions in muscle mass resulting from the loss of nNOS were not solely due to decreased body mass. (**F**) Mean myofiber Feret diameter from wild-type, mdx and DKO TA muscles. As expected, the mean mdx myofiber Feret diameter was larger than wild-type controls reflecting bigger muscle cells; however this increase was prevented in DKO muscles. (**G**) The range of Feret diameters represented in box and whisker plots in wild-type, mdx and DKO groups. Boxes (25th–75th percentile) contain median (horizontal bar) values. The whiskers represent minimum and maximum Feret diameters and the medians of each group are compared. The median and range of myofiber Feret diameters were increased in dystrophin-null TA muscles indicating compensatory hypertrophy in mdx mice. Decreases Feret diameter spread as well as median Feret diameter showed that the hypertrophic growth of mdx muscle was prevented by nNOSμ and nNOSβ depletion. $^{*}P < 0.05$, $^{***}P < 0.001$. (A–E) $n = 19–24$ for each group. F, $n = 4$ per group.

number of larger fibers (Fig. 3G). In contrast, there was a reduction in median Feret diameter and downward box shift in DKO muscles relative to wild-type and mdx controls reflecting a population of muscle fibers with smaller fiber diameter (median Feret diameters: WT, 72 μm; mdx, 89 μm, DKO, 53 μm). Given that nNOSμ has been previously shown to be dispensable for compensatory growth, these findings suggest that nNOSβ is necessary for the compensatory hypertrophy of mdx muscle cells.

### Loss of nNOS reduces central nucleation and promotes macrophage infiltration without impacting hyperCKemia in mdx mice

Increased numbers of central nucleated myofibers is a well-established pathological biomarker of dystrophin-deficient muscle, marking myofibers that have undergone a degeneration and regeneration event. NO therapies have discordant effects on central nucleation and the loss of nNOSμ has no impact on central nucleation in mdx mice (9,21,22,25,30–32). To determine the impact of the absence of all nNOS activity on central nucleation, we determined the fraction of myofibers with centrally localized nuclei in whole-muscle sections from wild-type, mdx and DKO mice (Fig. 4). As expected, wild-type TA muscles have few centrally nucleated myofibers (2.5%) compared with mdx mice (63.5%) (Fig. 4A and B). Interestingly, a 32% reduction in centrally nucleated muscle cells occurred in DKO mice (Fig. 4A and C). The reduction in central nucleation could indicate a beneficial reduction in muscle degeneration or damage or a deleterious reduction in muscle cell regeneration. To explore these possibilities, we evaluated serum creatine kinase activities. As expected, mdx mice exhibit significant hyperCKemia; however, the loss of nNOS did not impact

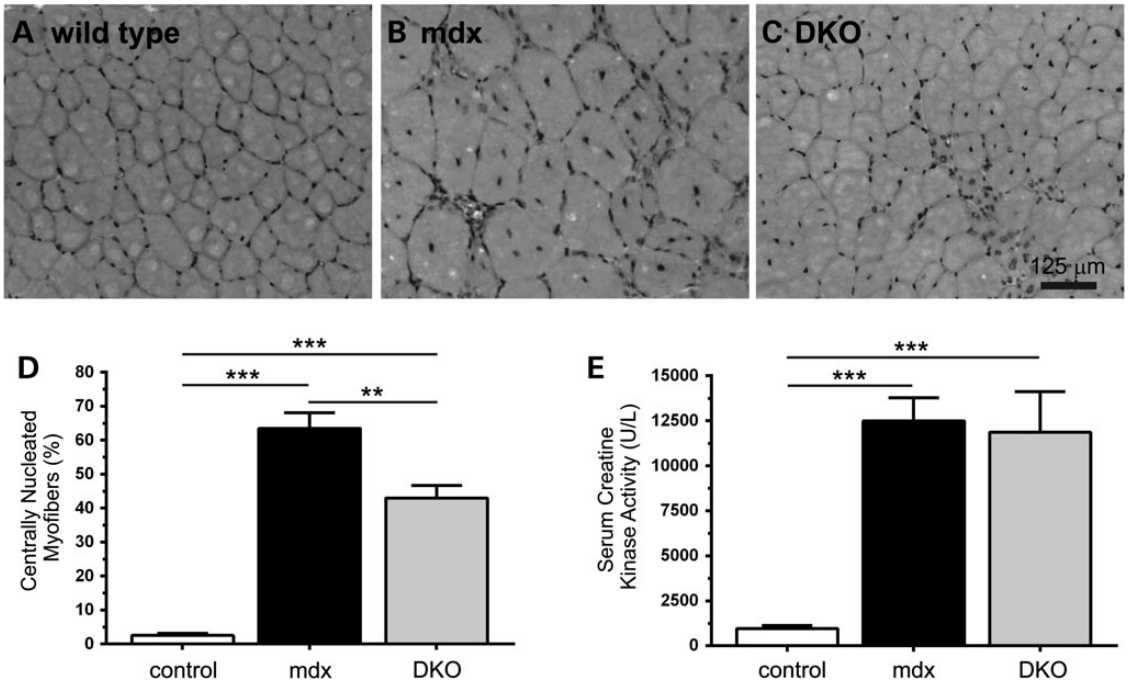


**Figure 4.** nNOS depletion reduces mdx muscle central nucleation without impacting hyperCKemia. (**A** and **B**) Dystrophin-deficient muscle exhibit a stereotypical increase in the fraction of muscle cells with centrally localized nuclei indicating that those myofibers have undergone degeneration and/or regeneration. Representative hematoxylin (nuclei stain) and eosin (cytoplasm stain) labeled muscle sections from mdx tibialis anterior muscles show a stereotypical elevation of centrally localized nuclei compared with wild-type controls. (**C**) Loss of both nNOSβ and nNOSμ decreased the fraction of myofibers with centrally localized nuclei suggesting perturbation of mdx muscle cell degeneration/regeneration. (**D**) Quantitation of the decrease in central nucleation in DKO mice. (**E**) Persistent elevated serum creatine kinase activities (hyperCKemia) in mdx mice marking extensive muscle damage and turnover. HyperCKemia in DKO mice was not different from mdx controls. $^{**}P < 0.01$, $^{***}P < 0.001$. (A–D), $n \geq 4$ per group. E, $n = 15$, 17 and 11 for wild-type, mdx and DKO groups, respectively.

elevated serum creatine kinase activities in DKO mice (Fig. 4C). These data indicate sustained high levels of muscle damage in DKO mice consistent with the possibility that decreased central nucleation results from reduced regeneration, not a reduction in degeneration.

Additional evidence that loss of nNOS prevented muscle regeneration came from observations of increased focal inflammation in DKO muscle (Fig. 5). As expected, wild-type TA muscles showed no overt inflammation (Fig. 5A, D and G). In contrast, significant accumulation of inflammatory cells occurred in mdx TA muscles (Fig. 5B and E). Remarkably, focal inflammatory cell infiltration was substantially exacerbated in DKO muscle, with high densities of inflammatory cells covering areas of muscle that were on average ∼11-fold greater in DKO than in mdx muscle (Fig. 5C and G). We then sought to confirm that the infiltrating cells were indeed immune cells. Given that nNOSα opposes macrophage infiltration in mdx muscles, we tested the hypothesis that the suspected infiltrating immune cells in DKO muscles were in fact macrophages (21) (Fig. 5H). Macrophages were identified by anti-CD68 antibody immunolabeling. While few macrophages could be identified in wild-type muscle, large numbers of CD68-positive macrophages were observed in mdx muscle as expected (Fig. 5H, top and middle rows, respectively). Furthermore, very high densities of CD68-positive macrophages accumulated at the same sites where large numbers of infiltrating cells could be observed by hematoxylin and eosin labeling (Fig. 5H, bottom row). This suggested that the majority of infiltrating immune cells in DKO muscles were indeed macrophages. Furthermore, given that loss of nNOSμ was reported previously to have no impact on inflammatory cell infiltration, these data suggest that nNOSβ can modulate the magnitude of the inflammatory response in dystrophin-null muscle (30–32).

### Elimination of nNOSβ and nNOSμ exacerbates muscle weakness in mdx mice

To determine whether exacerbated muscle damage in DKO mice was accompanied by exaggerated muscle weakness, we examined tetanic force output of DKO muscles under both isometric and eccentric conditions. TA muscles from wild-type, mdx and DKO mice exhibited similar normalized tetanic force generating capacity between stimulation frequencies of 10–200 Hz (Fig. 6A). Wild-type and mdx muscles also exhibited comparable maximal isometric tetanic force output capacity (Fig. 6B). However, consistent with reduced myofiber size, DKO muscles had markedly reduced maximal tetanic force output. Importantly, deficits in maximal force output were not entirely due to reductions in muscle size, because mean specific force (maximal tetanic force output normalized to muscle cross-sectional area) was also significantly decreased in DKO TA muscle ($148 \pm 6$ kN/m$^2$) compared with mdx ($173 \pm 4$ kN/m$^2$) and wild-type ($231 \pm 5$ kN/m$^2$) controls (Fig. 6C). mdx muscles showed stereotypical reductions in specific force, marking intrinsic muscle weakness compared with wild-type controls

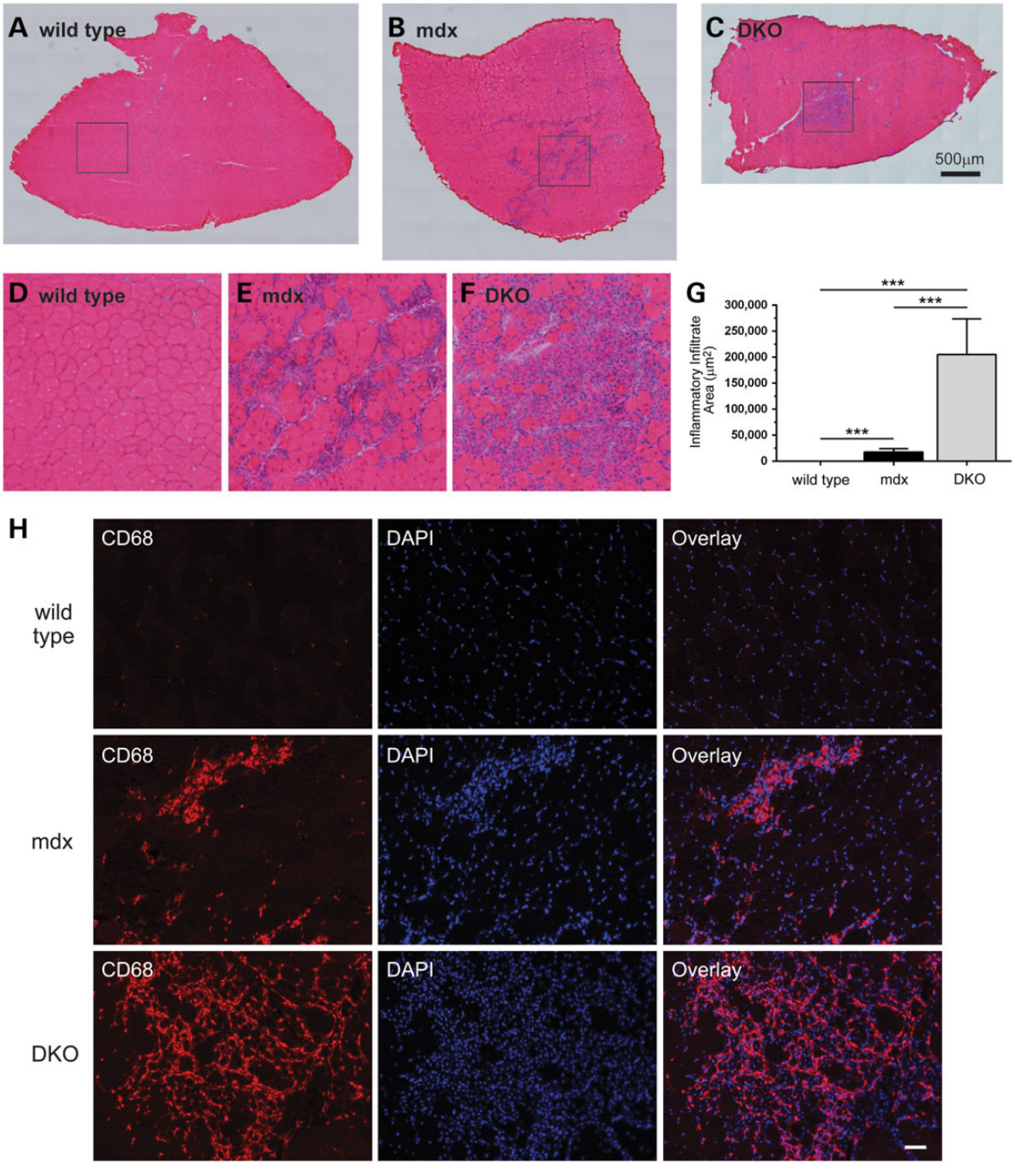


**Figure 5.** Elimination of nNOSβ and nNOSμ promotes macrophage infiltration in mdx skeletal muscle. We investigated the extent of inflammatory cell influx in wild-type, mdx and DKO tibialis anterior skeletal muscles using hematoxylin and eosin staining. (**A**–**C**) Representative images constructed by automated image tiling of whole sections from the midbelly of tibialis anterior muscles are shown. (A) Control muscles exhibit no significant inflammation. (B) As expected mdx muscles show pronounced inflammatory cell infiltration. (C) DKO tibialis muscles exhibited large areas of focal inflammatory cell accumulation marking exacerbated inflammation. (**D**–**F**) These images represent the magnified areas within the boxes of A, B and C, respectively. (**G**) Quantitation of inflammatory cell infiltration areas reveals an extensive increase in focal inflammatory cell infiltration in DKO muscle compared with mdx and wild-type controls. (**H**) To provide evidence that these infiltrating cells were macrophages, muscle sections were labeled with anti-CD68 antibody and nuclei counterstained with DAPI. Very few CD68-positive cells could be observed in wild-type muscle (H, top row). However, large numbers of CD68-positive macrophages were observed in mdx muscles as expected (**H**, middle row). nNOS depletion from mdx muscles increased numbers of CD68-positive macrophages in DKO muscles indicating greater focal inflammation (H, bottom row). These data suggest an important anti-inflammatory role for nNOS splice variants in dystrophin-deficient skeletal muscle. $^{***}P < 0.001$ from one-way ANOVA analysis and Bonferrroni multiple comparison tests. For wild-type, mdx and DKO groups, $n \geq 4$. Scale bar in H, 50 μm.

(Fig. 6C). These data suggest that nNOS depletion exacerbates skeletal muscle weakness in mdx mice.

To further understand the impact of nNOS deficiency on contractility, we investigated the regulation of muscle fatigue by nNOS in mdx mice which remains unknown. Contraction-induced muscle fatigue is not to be confused with previously reported ‘exaggerated fatigue’ or ‘postexercise inactivity’ in mdx mice which is poor recovery of cage ambulatory activity

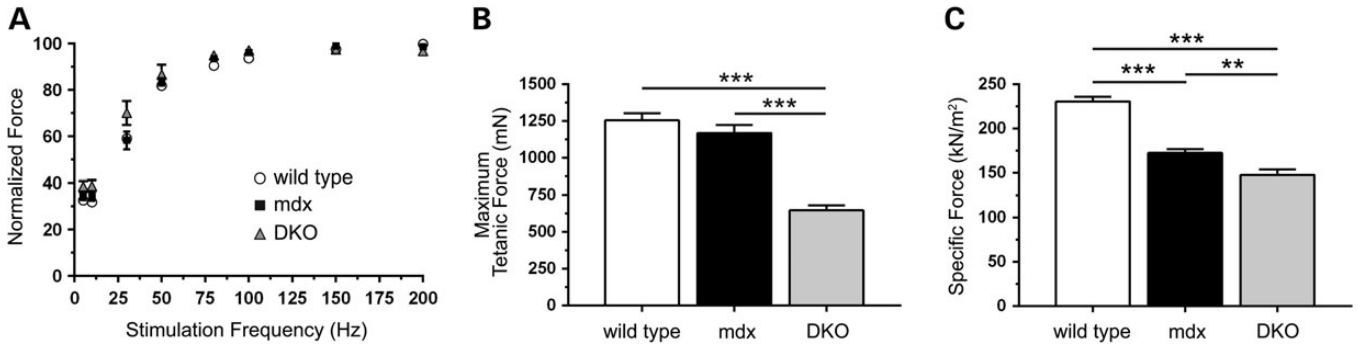


**Figure 6.** nNOSβ and nNOSμ depletion exacerbates mdx muscle weakness. The impact of nNOS depletion on the isometric tetanic contractile properties of mdx tibialis anterior (TA) muscles was determined *in situ*. (**A**) wild-type, mdx and nNOS-deficient mdx muscles exhibited similar normalized tetanic force outputs across a wide range of stimulation frequencies. (**B**) Maximal tetanic force generation capacity in mdx TA muscles was comparable to wild-type. In contrast, DKO muscles displayed a 45 and 48% reduction in maximal tetanic force generating capacity compared with mdx and wild-type controls, respectively. (**C**) As expected, mdx TA muscles exhibited a significant 25% decrease in specific force (maximal tetanic force normalized to cross-sectional area) compared with wild-type controls. mdx muscle-specific force deficits were further exacerbated by the loss of nNOS. Thus, force deficits in DKO muscle reflect intrinsic muscle weakness and are not due to decreased muscle mass. $^{**}P < 0.01$, $^{***}P < 0.001$. For wild-type, mdx and DKO groups: $n = 15$, 15 and 10 in A; $n = 12$, 13 and 10 in B; $n = 12$, 15 and 11 in C, respectively.

after mild running exercise (5). Therefore, we evaluated TA muscle fatigue resistance in wild-type, mdx and DKO mice *in situ*. Loss of dystrophin significantly reduced contraction-induced fatigue resistance and inhibited force recovery (∼14% force deficit) at 1 min compared with controls (Fig. 7). However, force output was similar to controls after a 5 min rest period indicating a full recovery from fatigue. Unexpectedly, DKO muscle fatigue was similar to mdx controls. This was surprising since we reported that loss of nNOS activity causes severe contraction-induced fatigue and inhibits force recovery in non-dystrophic mice (28). Like mdx muscles, DKO muscles also showed poor force recovery at 1 min compared with wild-type controls. Thus, both mdx and DKO muscles are slower to recover muscle strength after exercise marking exaggerated muscle fatigue. Postexercise inactivity in mdx mice has been attributed to loss of nNOSμ-modulated blood flow regulation (5). However, our data suggest that exaggerated muscle fatigue also may contribute to postexercise inactivity (Fig. 7). Furthermore, and contrary to expectations, these intriguing findings suggest the existence of compensatory mechanisms that preserve muscle fatigue resistance in mdx mice in the absence of nNOS.

Next, we investigated muscle force output under eccentric (lengthening) conditions. Dystrophin-deficient muscles exhibit a hallmark susceptibility to eccentric contraction-induced injury which plays an important role in pathogenesis (40–42). To determine whether nNOS–NO could modulate contraction-induced damage, TA muscles from wild-type, mdx and DKO mice were subjected to a series of eccentric contractions at increasing lengths or percent stretch (Fig. 8). mdx muscles exhibited force deficits at 25% stretch that became progressively larger at longer lengths relative to wild-type (Fig. 8). DKO muscles showed greater force deficits at shorter and more physiologically relevant stretches compared with mdx and wild-type controls (Fig. 8). Thus, consistent with our findings of increased muscle damage in DKO mice, nNOS may modulate the severity of eccentric contraction-induced damage in dystrophin-null muscle. Since others have shown that loss of nNOSμ has no impact on force output during eccentric contractions, these findings suggest nNOSβ may modulate eccentric contraction-induced muscle damage in mdx mice (32). Overall, these data provide compelling evidence that nNOS pathways modulate both isometric and eccentric force production in dystrophin-deficient skeletal muscle.

## DISCUSSION

The overarching finding of this study is that nNOS has a more multifaceted role in modulating the clinically relevant features of dystrophic muscle pathogenesis than previously recognized. This broader role is likely attributable in large part to nNOSβ which appears to play key roles in compensatory hypertrophy, inflammation and eccentric contraction-induced muscle damage in dystrophin-deficient muscle. These findings suggest that nNOSβ should be considered when accounting for the benefits of NO in mdx mice. In addition, they suggest nNOSβ be investigated as a therapeutic target for mitigating muscle damage and weakness in dystrophinopathies.

In addition, dystrophin-deficiency disrupted subsarcolemmal Golgi-nNOSβ localization and prevented normal association of nNOSβ with the *cis*-Golgi compartment. Thus, loss of dystrophin disrupted the spatial control of nNOSβ signaling. It is likely that destabilization of the subsarcolemmal microtubule cytoskeleton that scaffolds Golgi membranes is a causal factor in the mislocalization of Golgi-nNOSβ in mdx muscle (34). Since it is firmly established that loss of dystrophin also causes nNOSμ mislocalization, dystrophin deficiency thus appears to globally disrupt the spatial control of NO signaling by preventing correct localization of both nNOSμ and nNOSβ (3,7,8). The tight control of NO synthesis sites is a critical regulatory mechanism for facilitating specific and efficient NO signal propagation (43,44). Disruption of nNOSβ signaling in this way could exacerbate dystrophic disease severity, just as nNOSμ mislocalization prevents it from promoting blood delivery to active muscle (16). Consistent with this possibility, microdystrophin expression in mdx muscle reduces dystrophic pathology and rescues defective Golgi localization (34). Thus, it is likely that microdystrophin also rescued Golgi-nNOSβ localization and improved spatial control of subsarcolemmal NO signaling.

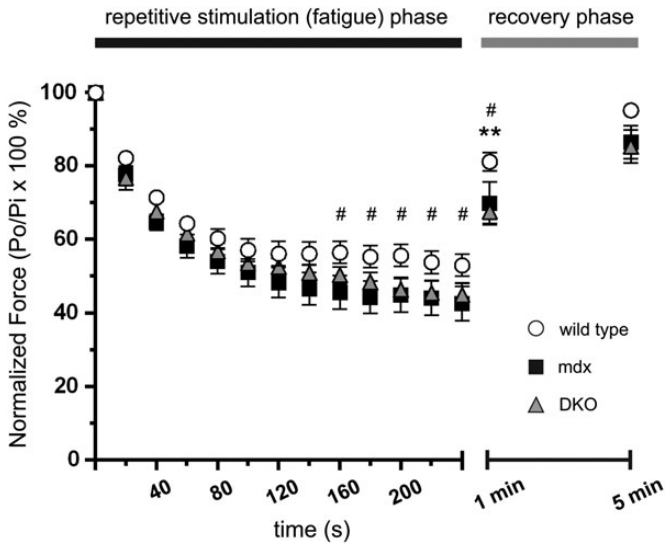


**Figure 7.** mdx muscles are protected from exaggerated muscle fatigue caused by nNOS deficiency. The fatigue resistance of tibialis anterior muscles in wild-type, mdx, and DKO mice was determined *in situ*. After 160 s of repetitive stimulation, mdx muscles exhibited mild but significant force deficits compared with wild-type controls, indicating reduced fatigue resistance. Surprisingly, DKO muscles exhibited similar force deficits to mdx muscle. At 1 min into the recovery phase, both mdx and DKO TA muscles exhibited significant postexercise weakness (14 and 17% respectively) compared with wild-type TA controls. However, full force recovery was observed after 5 min of rest confirming that force defects were reversible and not due to contraction-induced damage. $^{\#}P < 0.05$ wild-type versus mdx. $^{*}P < 0.05$ wild-type versus DKO. $n = 10$, 6 and 7, for wild-type, mdx and DKO groups, respectively.

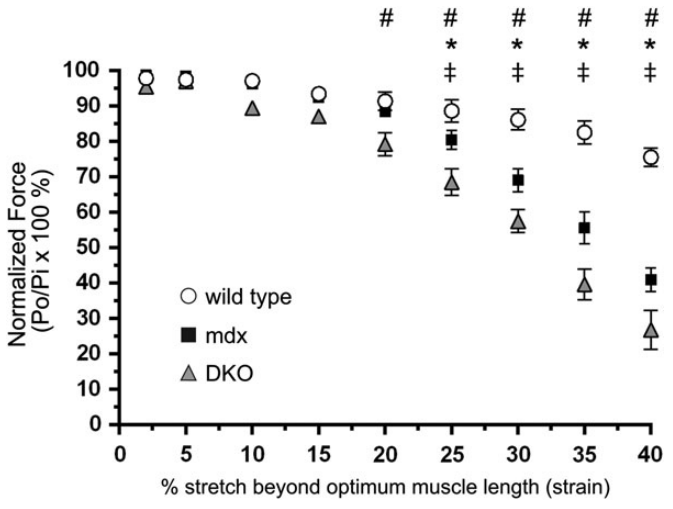


**Figure 8.** Loss of nNOS from dystrophin-null muscle exacerbates eccentric contraction-induced muscle damage. To determine whether nNOS elimination from mdx muscle impacted eccentric contraction-induced muscle damage, TA muscles from wild-type, mdx and DKO mice were subjected to a series of lengthening contractions of progressively increasing lengths (stretch) *in situ*. At stretches beyond 25%, mdx muscle exhibited reduced force output compared with wild-type controls. Force deficits were exacerbated in DKO muscles at strains beyond 20%. This suggested DKO mice had an increased susceptibility to eccentric contraction-induced damage. $^{*}P < 0.05$ wild-type versus mdx. $^{\#}P < 0.05$ wild-type versus DKO. $^{\ddagger}P < 0.05$ mdx versus DKO. $n = 7$, 8 and 7, for wild-type, mdx and DKO groups, respectively.

While the impact of disrupted nNOSβ signaling on dystrophic pathology remains to be directly determined, our data suggest that nNOSβ may be necessary for compensatory muscle hypertrophy in mdx mice. This finding is consistent with reports suggesting a role for NO and nNOS in muscle hypertrophy in wild-type mice (28,35,36,45). mdx muscles undergo a well-established compensatory hypertrophy, so that total tetanic force output is comparable between young adult wild-type and mdx muscle (37). This compensatory muscle growth does not occur in human or canine dystrophin-null muscle; therefore the murine pathways responsible represent potential therapeutic targets for attenuating muscle wasting in DMD patients (37,38). Three independent studies have reported that nNOSμ null mdx muscles show no change in muscle cell growth (30–32). These reports, together with our current findings, suggest that nNOSβ is necessary for the compensatory growth of mdx muscle. These data support further investigation of nNOSβ as a target for decreasing dystrophin-deficient muscle wasting.

Our data also suggest nNOSβ modulates inflammation in dystrophic muscle. DKO muscles showed a remarkable increase in focal macrophage cell infiltration supporting the possibility that nNOS pathways oppose muscle inflammation in mdx mice (21). A prominent cellular immune response, that includes infiltration of macrophages and other immune cell classes, is an important pathogenic feature of dystrophin-deficient skeletal muscle, even at asymptomatic stages of disease progression (21,46–48). Consistent with our findings, skeletal muscle-specific expression of the nNOSα splice variant markedly decreased inflammatory cell infiltration and concomitant muscle cell breakdown (21). Amplification of NO–cGMP signaling also suppresses TNFα expression providing additional support for an anti-inflammatory role for nNOS in dystrophic muscle (25).

Increased inflammation was accompanied by decreases in central nucleation and high levels of serum creatine kinase activity. Collectively, these data argue that the loss of nNOS exacerbated muscle damage in agreement with previous reports suggesting that NO can both reduce muscle cell degeneration and enhance regeneration (13,21,22). In addition to a possible anti-inflammatory role, these data also suggest nNOSβ may modulate muscle integrity, because loss of residual nNOSμ expression has no overt impact on inflammation, central nucleation or muscle damage in mdx mice (30–32). These findings provide a new conceptual framework for understanding the emerging roles of NO in the modulation of dystrophic muscle damage and repair (13).

The loss of muscle integrity in DKO mice coincided with several intriguing and unexpected effects on muscle contractile performance. First, DKO muscles displayed significant reductions in maximum isometric tetanic which were due to the significant reduction in muscle mass and myofiber size. However, specific force was also decreased in DKO muscles relative to mdx controls indicating that intrinsic muscle weakness was not due to muscle atrophy. In contrast, treatment of mdx mice with 7-NI, a selective nNOS inhibitor, was reported to enhance specific force in dystrophin-null muscles, as was the genetic depletion of nNOSμ (32). The reasons for this discrepancy are unclear and remain to be determined in future studies. However, possible reasons may include strain and genetic differences between mdx mouse models and that 7-NI is not an effective inhibitor of nNOSβ activity *in vivo*.

Further unappreciated complexity of nNOS function in mdx muscle was revealed by the observation that nNOS depletion did not affect the exaggerated muscle fatigue of mdx mice. While 'fatigue' or exercise intolerance is well-established characteristics of mdx mice and Duchenne patients, the mechanisms responsible remain unclear. However, loss of sarcolemmal nNOSμ regulation of blood delivery to active muscles is thought to play an important role although loss of sarcolemmal nNOSμ-mediated blood flow has no impact on muscle strength or fatigue resistance (5,28). Our data suggest an additional mechanism where exaggerated muscle fatigue and slow force recovery in limb muscles after repetitive use also contributes to exercise intolerance and postexercise inactivity in mdx mice (5,49,50). These findings argue that the loss of sarcolemmal nNOSμ control of blood flow is not the sole factor contributing to postexercise inactivity in mdx mice.

Our data also suggest that muscle fatigue, is a pathogenic feature of dystrophin-deficient muscle, although previous reports are conflicting. The mdx mouse diaphragm, which best recapitulates the severity of human pathology, exhibits significant contraction-induced muscle fatigue; however, excised EDL and soleus muscles that lack normal blood supply show normal fatigue resistance (25,51,52). It is widely accepted that the most physiologically informative way to study fatigue is in a blood-perfused system *in situ* or *in vivo* (53). Discrepancies between blood delivery and oxygen concentrations *in vitro* and our *in situ*/*in vivo* studies of fatigue in hindlimb muscles from mdx mice may be one reason why hindlimb muscles show normal fatigue resistance *in vitro*.

Our finding that loss of all nNOS activity in mdx muscle had no impact on fatigue resistance was in sharp contrast to previous findings (14). Muscles lacking nNOSμ alone or both nNOSμ and nNOSβ exhibit poor muscle fatigue resistance (28,45). Therefore, we anticipated a decrease in muscle fatigue resistance in DKO mice. However, the role of nNOS in muscle fatigue appears to differ between dystrophic and normal muscle environments. Our data indicate the existence of a latent compensatory change in dystrophin-deficient muscle that preserves fatigue resistance in the absence of nNOS. Understanding how muscle fatigue resistance can be preserved in the absence of nNOS has important implications for therapies to fight exercise intolerance in dystrophinopathies.

The surprising effects of nNOS deficiency on mdx muscle contractility were not confined to fatigue. nNOSμ and nNOSβ depletion from dystrophin-null muscle also exacerbated muscle damage and force loss during eccentric contractions. The susceptibility of dystrophin-deficient muscle to eccentric contraction-induced damage is a well-established feature of mdx pathology (40–42). In non-dystrophic skeletal muscles, loss of nNOSμ alone or both nNOSμ and nNOSβ has no impact on force output during eccentric contractions suggesting that nNOS does not normally regulate lengthening contraction force output (28,45). Similarly, loss of nNOSμ from dystrophin-deficient muscle also has no impact on force production during eccentric contractions (32). Taken together these findings suggest that loss of nNOSβ promotes contraction-induced muscle damage in DKO mice and that nNOSβ activity modulates the ability of dystrophin-deficient muscle to generate force during lengthening contractions.

At this stage, we may only speculate about how the loss of nNOSβ exacerbates eccentric contraction-induced muscle damage. It may do so by exacerbating subsarcolemmal microtubule instability; thereby promoting a loss of mdx muscle structural integrity (34). Loss of nNOSμ and nNOSβ, but not nNOSμ alone, disrupts subsarcolemmal microtubules (28). These data are consistent with an *in vivo* role for NO-mediated *S*-nitrosation of tubulin which is thought to regulate tubulin polymerization and microtubule stability (54,55). Thus, microtubule lattice defects may be compounded by the loss of both dystrophin and nNOS which together drive microtubule instability which may in turn exacerbate contraction-induced damage (34,56).

DKO muscles also may exhibit enhanced microtubule-dependent activation of NADPH oxidase to synthesize superoxide, which promotes pathogenic $Ca^{2+}$ influx through TRPC channels during eccentric contractions (57–61). NO-mediated cysteine nitrosation inhibits superoxide generation by NADPH oxidase (57). Thus, loss of subsarcolemmal nNOSβ activity in mdx mice may promote eccentric contraction-induced damage by exacerbating microtubule instability and deregulating NADPH oxidase superoxide synthesis. Importantly, these possible deleterious effects occurring on the sarcolemmal space are in excellent agreement with the importance of the tight spatial control of NO synthesis. Thus, exaggerated contraction-induced injury and concomitant weakness in DKO muscle may result from both signaling and structural defects.

In conclusion, this study provides several new insights into NO signaling in dystrophin-deficient skeletal muscle. First, the loss of dystrophin appears to globally disrupt the spatial control of nNOS splice variant signaling in mdx muscle. Second, NO has a more multifaceted role in modulating dystrophic muscle damage and force-generating capacity than previously recognized. These findings provide a new framework for understanding nNOS signaling in dystrophic muscle and strengthen the case for targeting NO pathways clinically. Indeed, our data suggest that the potential of NO-based therapies to ameliorate dystrophin-deficient muscle pathology is yet to be fully realized. This expansion of the role of NO is primarily attributable to the activity of the novel nNOSβ signaling pathway in skeletal muscle. Thus, this study identifies nNOSβ as a potential new drug target for NO-based therapy of DMD.

## MATERIALS AND METHODS

### Generation of nNOS-deficient mdx mice

All experimental procedures performed on mice were approved by the Institutional Animal Care and Use Committees of the Universities of Washington and Miami. nNOS-deficient mdx double knockout mice were made by breeding dystrophin-null ($DMD^{-/-}$) mdx mice with heterozygous nNOS ($NOS1^{-/-}$) knockout mice to generate double knockout (DKO) mice. mdx mice are the well-characterized C57BL/10ScSn-$Dmd^{mdx}$/J line (62). nNOS ($NOS1^{-/-}$) knockout mice are in a C57Bl6/J background and were generated by targeted deletion of exon 6 of the *NOS1* gene that inhibits expression of active nNOSμ and nNOSβ in skeletal muscle (28,39). Mice lacking a functional copy of the *NOS1* gene are infertile, precluding direct breeding of homozygous null animals (39). Therefore, $DMD^{-/-}$/$NOS1^{+/-}$ mice were interbred to create $DMD^{-/-}$/$NOS1^{-/-}$ DKO mice on a mixed C57Bl6-C57/Bl10 background. Comparisons of mdx and DKO phenotypes were made between age-and

strain-matched littermates. Wild-type C57/Bl6/J controls are included for reference. The wild-type muscle properties of interest here do not differ significantly between C57/Bl10, C57/Bl6 and mixed C57Bl6-C57/Bl10 backgrounds (25,28).

### Immunofluorescence labeling and confocal microscopy of myofibers

The method used to immunolabel the Golgi complex in single myofibers has been described (34). Briefly, gastrocnemius muscles from immature 2 and adult 8-week-old wild-type and mdx mice were freshly dissected, pinned out on sylgaard-coated dishes and fixed in 2% paraformaldehyde for 1 h. Muscles were rinsed 3 times with phosphate-buffered saline (PBS) then incubated in a PBS-based blocking buffer (50 mM glycine, 0.25% bovine serum albumin, 0.02% sodium azide, 0.04% saponin). Single and small groups of fibers were physically separated using fine forceps. Pre-blocked myofibers were incubated with primary antibodies diluted in blocking buffer overnight at 4°C. FITC-conjugated GM130 primary antibodies (Transduction Laboratories) were used to label the *cis*-Golgi compartment. Pan-specific nNOS amino (Invitrogen) and a carboxyl (Sigma-Aldrich) terminal rabbit polyclonal antibodies were used to label Golgi-targeted nNOSβ. Myofiber preparations were subsequently washed three times in blocking buffer. Myofibers labeled with nNOS antibodies were incubated with Rhodamine Red-X-conjugated donkey anti-rabbit secondary antibody (Jackson Immunoresearch Laboratories) for 1 h at room temperature, followed by three washes in blocking buffer. Labeled myofibers were mounted in ProLong® Gold antifade mounting medium containing DAPI (Invitrogen) to counterstain nuclei. Confocal microscopy was performed using a Leica TCS SP microscope equipped with a two photon UV laser used to excite DAPI (W. M. Keck Center for Advanced Studies in Neural Signaling, University of Washington).

### Image analysis of Golgi-nNOSβ localization

To determine the impact of dystrophin deficiency on the localization of Golgi-nNOSβ, we measured subsarcolemmal Golgi-nNOSβ densities (the number of puncta positive for both nNOSβ and GM130 per 1000 $\mu m^2$) as previously described (34). Briefly, the subsarcolemmal space of myofibers which contained the vast majority of nNOSβ and GM130-positive Golgi puncta was imaged in a single 0.427 μm deep (100 × NA 1.4 objective) optical section captured with a Leica SP2 confocal microscope. At least 24 individual myofibers per group were optically sectioned and quantitated. To calculate densities, nNOSβ and GM130-positive puncta were counted manually, normalized to myofiber cross-sectional area ($\mu m^2$), then multiplied by 1000. Cross-sectional area was determined by manually outlining myofiber perimeter, thereby creating a region of interest whose area was calculated using spatially calibrated Image J 1.46r software (63).

### Histological analyses of myofiber size, central nucleation and inflammation

To determine the impact of nNOS deficiency on mdx muscle size, freshly dissected tibialis anterior and soleus muscles isolated from adult 8-week-old mice were weighed and normalized to body mass. Note that muscles used for histological analyses were not used for functional tests. Feret diameters were determined in sections of tibialis anterior muscles dissected from adult mice and flash-frozen in liquid-nitrogen-cooled isopentane. Frozen 10 μm thick sections from the muscle midbelly were prepared with a Leica CM1860 cryostat then stained with hematoxylin and eosin using our published methods (25,28). Images of entire muscle cross sections were stitched together from individual image files captured sequentially at 10 × magnification with a DP80 digital camera (Olympus) and an automated tiling system (Olympus BX50 upright microscope fitted with a Prior Scientific motorized x-y stage). The Feret diameters of between 500 and 750 myofibers were determined from at least 4 mice per group using Image J 1.46r software (63). Feret's diameter is the longest distance between any two points along the myofiber selection boundary and is a reliable measure of muscle cell size since it is less susceptible to sectioning angle (64). The fraction of muscle cells with centrally localized nuclei, was performed as previously described (25). Inflammatory cell infiltrates were detected histologically in frozen cryosections by hematoxylin/eosin staining. The areas of muscle ($\mu m^2$) covered by infiltrating inflammatory cells were measured manually using spatially calibrated Image J 1.46r software and were used as an index of inflammation. Areas were measured from 3–4 tiled images of whole tibialis anterior cross sections from the muscle midbelly from at least four mice. The lysosomal protein CD68 is highly enriched in macrophages that represent the predominant inflammatory cell type in mdx muscle tissue; therefore a rat anti-mouse CD68 (clone FA-11) antibody (AbD Serotec) was used as a macrophage marker (65). Macrophage labeling was performed on tibialis anterior cryosections fixed with 1% paraformaldehyde for 30 min and permeabilized with 0.1% Triton X-100 for 5 min. Sections were blocked in 3% bovine serum albumin in PBS for 20 min then incubated with rat anti-mouse CD68 for 3 h at 4°C. After washing in PBS, sections were incubated with Rhodamine Red™-X-conjugated donkey anti-rat secondary antibodies for 1 h at room temperature. 5 μM DAPI in PBS was then incubated on sections for 10 min then rinsed off with PBS. Slides were mounted in ProLong® Gold antifade medium (Invitrogen) and imaged on a Olympus BX50 upright fluorescence microscope.

### HyperCKemia measurements

HyperCKemia was evaluated using serum creatine kinase activity assays. Blood was collected from 8-week-wild-type, mdx and DKO old mice and serum creatine kinase activities were measured according to the manufacturer's instructions (Stanbio Laboratory).

### *In situ* analysis of skeletal muscle contractile function

Tests of muscle contractile performance were performed on the tibialis anterior (TA) muscle in anesthetized 8-week-old adult mice as described (45). Mice were anesthetized with intraperitoneal injections of 2,2,2, tribromoethanol (Sigma-Aldrich). Mice were positioned on a 37°C heated platform and the distal tendon of the TA muscle was attached to the lever arm of a servomotor (Model 305B-LR, Aurora Scientific). The exposed muscle surface was kept moist by application of prewarmed isotonic saline. TA muscle contractions were driven by electrical stimulation of the peroneal nerve. The muscle was adjusted to an

optimum length ($L_o$) that produced the maximum twitch force ($P_t$). While held at $L_o$, the TA was tetanically stimulated every 2 min from 5 to 200 Hz to evaluate any potential dependence force output on stimulation frequency. Maximal tetanic force ($P_o$) generation was typically achieved at 200 Hz and was used to normalize force output over the 5–200 Hz range. After the completion of testing, both $L_o$ and TA mass were recorded and used to calculate specific tetanic ($sP_o$) force. To test the capacity of muscle to resist contraction-induced fatigue, TA muscles were subjected to 4 min of repeated maximal tetanic contractions. Muscles were stimulated (40 V, 200 Hz, 300 ms) every 2 s intervals for 4 min and maximum isometric tetanic force production was recorded. To ensure force loss was reversible and not due to muscle damage, recovery from fatigue was assessed by recording force output ($P_o$) at 1 min and 5 min after the completion of the fatigue period.

The ability of TA muscles to maintain force output during eccentric contraction was assessed by subjecting them to consecutive maximal tetanic eccentric contractions of progressively increased strain applied at the rate of two fiber lengths/s. Strain is the percentage increase in length beyond the optimal muscle length $L_o$. Muscles were maximally tetanically stimulated (4 V, 200 Hz) for 150 ms at fixed length to achieve maximal isometric tension, immediately followed by a 200 ms stimulation during the application of a 0–45% length increase beyond $L_o$. Lengthening contractions were conducted at 1 min intervals to eliminate the confounding impact of fatigue on force-generating capacity. The maximum tetanic force generated prior to the initiation of the subsequent lengthening contraction was recorded and normalized to the force of the first contraction.

### Statistical analyses

All values are reported as mean ± standard error of the mean, except for the box and whisker plots in Figure 3G which report median, 25 and 75 percentile (box) values, minimum and maximum values. Significant differences between medians were discerned by Mann–Whitney tests. Statistically significant differences between means of wild-type, mdx and DKO groups were determined by one-way ANOVA, followed by the Tukey multiple comparison post hoc tests between paired groups. Two-way ANOVAs were used for analysis of force output during fatigue and lengthening contraction protocols using time and genotype as variables and followed by Tukey multiple comparison post hoc tests between paired groups. Statistical calculations were performed using Prism version 4 software (Graphpad Software Inc.) $P$ values of $<0.05$ were considered significant.

## ACKNOWLEDGEMENTS

We thank Dr Kimberley Craven for critically editing the manuscript.

*Conflict of Interest statement*. None declared.

## FUNDING

Research reported in this publication was supported by the Muscular Dystrophy Association and by NIAMS of the National Institutes of Health under award numbers 69075 (JMP), NS33145 and AR056221 (SCF). SMR was supported by an American Physiological Society Undergraduate Summer Research Fellowship and Mary Gates Research Scholarship. The content is solely the responsibility of the authors and does not necessarily represent the official views of the National Institutes of Health.

## REFERENCES

1. Koenig, M., Hoffman, E.P., Bertelson, C.J., Monaco, A.P., Feener, C. and Kunkel, L.M. (1987) Complete cloning of the Duchenne muscular dystrophy (DMD) cDNA and preliminary genomic organization of the DMD gene in normal and affected individuals. *Cell*, **50**, 509–517.
2. Hoffman, E.P., Brown, R.H. Jr and Kunkel, L.M. (1987) Dystrophin: the protein product of the Duchenne muscular dystrophy locus. *Cell*, **51**, 919–928.
3. Brenman, J.E., Chao, D.S., Xia, H., Aldape, K. and Bredt, D.S. (1995) Nitric oxide synthase complexed with dystrophin and absent from skeletal muscle sarcolemma in Duchenne muscular dystrophy. *Cell*, **82**, 743–752.
4. Crosbie, R.H., Barresi, R. and Campbell, K.P. (2002) Loss of sarcolemma nNOS in sarcoglycan-deficient muscle. *FASEB J.*, **16**, 1786–1791.
5. Kobayashi, Y.M., Rader, E.P., Crawford, R.W., Iyengar, N.K., Thedens, D.R., Faulkner, J.A., Parikh, S.V., Weiss, R.M., Chamberlain, J.S., Moore, S.A. *et al.* (2008) Sarcolemma-localized nNOS is required to maintain activity after mild exercise. *Nature*, **456**, 511–515.
6. Finanger Hedderick, E.L., Simmers, J.L., Soleimani, A., Andres-Mateos, E., Marx, R., Files, D.C., King, L., Crawford, T.O., Corse, A.M. and Cohn, R.D. (2011) Loss of sarcolemmal nNOS is common in acquired and inherited neuromuscular disorders. *Neurology*, **76**, 960–967.
7. Brenman, J.E., Chao, D.S., Gee, S.H., McGee, A.W., Craven, S.E., Santillano, D.R., Wu, Z., Huang, F., Xia, H., Peters, M.F. *et al.* (1996) Interaction of nitric oxide synthase with the postsynaptic density protein PSD-95 and alpha1-syntrophin mediated by PDZ domains. *Cell*, **84**, 757–767.
8. Chang, W.J., Iannaccone, S.T., Lau, K.S., Masters, B.S., McCabe, T.J., McMillan, K., Padre, R.C., Spencer, M.J., Tidball, J.G. and Stull, J.T. (1996) Neuronal nitric oxide synthase and dystrophin-deficient muscular dystrophy. *Proc. Natl Acad. Sci. U.S.A.*, **93**, 9142–9147.
9. Asai, A., Sahani, N., Kaneki, M., Ouchi, Y., Martyn, J.A. and Yasuhara, S.E. (2007) Primary role of functional ischemia, quantitative evidence for the two-hit mechanism, and phosphodiesterase-5 inhibitor therapy in mouse muscular dystrophy. *PloS One*, **2**, e806.
10. Tidball, J.G. and Wehling-Henricks, M. (2007) The role of free radicals in the pathophysiology of muscular dystrophy. J. Appl. Physiol. *(1985)*, **102**, 1677–1686.
11. Wehling-Henricks, M., Oltmann, M., Rinaldi, C., Myung, K.H. and Tidball, J.G. (2009) Loss of positive allosteric interactions between neuronal nitric oxide synthase and phosphofructokinase contributes to defects in glycolysis and increased fatigability in muscular dystrophy. *Hum. Mol. Genet.*, **18**, 3439–3451.
12. Lai, Y., Thomas, G.D., Yue, Y., Yang, H.T., Li, D., Long, C., Judge, L., Bostick, B., Chamberlain, J.S., Terjung, R.L. *et al.* (2009) Dystrophins carrying spectrin-like repeats 16 and 17 anchor nNOS to the sarcolemma and enhance exercise performance in a mouse model of muscular dystrophy. *J. Clin. Invest.*, **119**, 624–635.
13. Rovere-Querini, P., Clementi, E. and Brunelli, S. (2013) Nitric oxide and muscle repair: multiple actions converging on therapeutic efficacy. *Eur. J. of Pharmacol.*, **730**, 181–185.
14. Percival, J.M. (2011) nNOS regulation of skeletal muscle fatigue and exercise performance. *Biophys. Rev.*, **3**, 209–217.
15. Thomas, G.D., Sander, M., Lau, K.S., Huang, P.L., Stull, J.T. and Victor, R.G. (1998) Impaired metabolic modulation of alpha-adrenergic vasoconstriction in dystrophin-deficient skeletal muscle. *Proc. Natl Acad. Sci. U.S.A.*, **95**, 15090–15095.
16. Thomas, G.D., Shaul, P.W., Yuhanna, I.S., Froehner, S.C. and Adams, M.E. (2003) Vasomodulation by skeletal muscle-derived nitric oxide requires alpha-syntrophin-mediated sarcolemmal localization of neuronal nitric oxide synthase. *Circ. Res.*, **92**, 554–560.

17. Firestein, B.L. and Bredt, D.S. (1999) Interaction of neuronal nitric-oxide synthase and phosphofructokinase-M. *J. Biol. Chem.*, **274**, 10545–10550.
18. Aquilano, K., Baldelli, S. and Ciriolo, M.R. (2014) Nuclear recruitment of neuronal nitric-oxide synthase by alpha-syntrophin is crucial for the induction of mitochondrial biogenesis. *J. Biol. Chem.*, **289**, 365–378.
19. Percival, J.M., Adamo, C.M., Beavo, J.A. and Froehner, S.C. (2011) Evaluation of the therapeutic utility of phosphodiesterase 5A inhibition in the mdx mouse model of Duchenne muscular dystrophy. *Handb. Exp. Pharmacol.*, **204**, 323–344.
20. Martin, E.A., Barresi, R., Byrne, B.J., Tsimerinov, E.I., Scott, B.L., Walker, A.E., Gurudevan, S.V., Anene, F., Elashoff, R.M., Thomas, G.D. *et al.* (2012) Tadalafil alleviates muscle ischemia in patients with Becker muscular dystrophy. *Sci. Transl. Med.*, **4**, 162ra155.
21. Wehling, M., Spencer, M.J. and Tidball, J.G. (2001) A nitric oxide synthase transgene ameliorates muscular dystrophy in mdx mice. *J. Cell Biol.*, **155**, 123–131.
22. Brunelli, S., Sciorati, C., D'Antona, G., Innocenzi, A., Covarello, D., Galvez, B.G., Perrotta, C., Monopoli, A., Sanvito, F., Bottinelli, R. *et al.* (2007) Nitric oxide release combined with nonsteroidal antiinflammatory activity prevents muscular dystrophy pathology and enhances stem cell therapy. *Proc. Natl Acad. Sci. U.S.A.*, **104**, 264–269.
23. Thomas, G.D., Ye, J., De Nardi, C., Monopoli, A., Ongini, E. and Victor, R.G. (2012) Treatment with a nitric oxide-donating NSAID alleviates functional muscle ischemia in the mouse model of Duchenne muscular dystrophy. *PloS One*, **7**, e49350.
24. Colussi, C., Mozzetta, C., Gurtner, A., Illi, B., Rosati, J., Straino, S., Ragone, G., Pescatori, M., Zaccagnini, G., Antonini, A. *et al.* (2008) HDAC2 blockade by nitric oxide and histone deacetylase inhibitors reveals a common target in Duchenne muscular dystrophy treatment. *Proc. Natl Acad. Sci. U.S.A.*, **105**, 19183–19187.
25. Percival, J.M., Whitehead, N.P., Adams, M.E., Adamo, C.M., Beavo, J.A. and Froehner, S.C. (2012) Sildenafil reduces respiratory muscle weakness and fibrosis in the mdx mouse model of Duchenne muscular dystrophy. *J.Pathol.*, **228**, 77–87.
26. Percival, J.M., Siegel, M.P., Knowels, G. and Marcinek, D.J. (2013) Defects in mitochondrial localization and ATP synthesis in the mdx mouse model of Duchenne muscular dystrophy are not alleviated by PDE5 inhibition. *Hum. Mol. Genet.*, **22**, 153–167.
27. Silvagno, F., Xia, H. and Bredt, D.S. (1996) Neuronal nitric-oxide synthase-mu, an alternatively spliced isoform expressed in differentiated skeletal muscle. *J. Biol. Chem.*, **271**, 11204–11208.
28. Percival, J.M., Anderson, K.N., Huang, P., Adams, M.E. and Froehner, S.C. (2010) Golgi and sarcolemmal neuronal NOS differentially regulate contraction-induced fatigue and vasoconstriction in exercising mouse skeletal muscle. *J. Clin. Invest.*, **120**, 816–826.
29. Baum, O., Schlappi, S., Huber-Abel, F.A., Weichert, A., Hoppeler, H. and Zakrzewicz, A. (2011) The beta-isoform of neuronal nitric oxide synthase (nNOS) lacking the PDZ domain is localized at the sarcolemma. *FEBS Lett.*, **585**, 3219–3223.
30. Crosbie, R.H., Straub, V., Yun, H.Y., Lee, J.C., Rafael, J.A., Chamberlain, J.S., Dawson, V.L., Dawson, T.M. and Campbell, K.P. (1998) mdx muscle pathology is independent of nNOS perturbation. *Hum. Mol. Genet.*, **7**, 823–829.
31. Chao, D.S., Silvagno, F. and Bredt, D.S. (1998) Muscular dystrophy in mdx mice despite lack of neuronal nitric oxide synthase. *J. Neurochem.*, **71**, 784–789.
32. Li, D., Yue, Y., Lai, Y., Hakim, C.H. and Duan, D. (2011) Nitrosative stress elicited by nNOSmicro delocalization inhibits muscle force in dystrophin-null mice. *J. Pathol.*, **223**, 88–98.
33. Eliasson, M.J., Blackshaw, S., Schell, M.J. and Snyder, S.H. (1997) Neuronal nitric oxide synthase alternatively spliced forms: prominent functional localizations in the brain. *Proc. Natl Acad. Sci. U.S.A.*, **94**, 3396–3401.
34. Percival, J.M., Gregorevic, P., Odom, G.L., Banks, G.B., Chamberlain, J.S. and Froehner, S.C. (2007) rAAV6-microdystrophin rescues aberrant Golgi complex organization in mdx skeletal muscles. *Traffic*, **8**, 1424–1439.
35. Sellman, J.E., DeRuisseau, K.C., Betters, J.L., Lira, V.A., Soltow, Q.A., Selsby, J.T. and Criswell, D.S. (2006) In vivo inhibition of nitric oxide synthase impairs upregulation of contractile protein mRNA in overloaded plantaris muscle. *J. Appl. Physiol.*, (1985), **100**, 258–265.
36. Ito, N., Ruegg, U.T., Kudo, A., Miyagoe-Suzuki, Y. and Takeda, S. (2013) Activation of calcium signaling through Trpv1 by nNOS and peroxynitrite as a key trigger of skeletal muscle hypertrophy. *Nat. Med.*, **19**, 101–106.
37. Lynch, G.S., Hinkle, R.T., Chamberlain, J.S., Brooks, S.V. and Faulkner, J.A. (2001) Force and power output of fast and slow skeletal muscles from mdx mice 6–28 months old. *J. Physiol.*, **535**, 591–600.
38. Cooper, B.J., Winand, N.J., Stedman, H., Valentine, B.A., Hoffman, E.P., Kunkel, L.M., Scott, M.O., Fischbeck, K.H., Kornegay, J.N., Avery, R.J. *et al.* (1988) The homologue of the Duchenne locus is defective in X-linked muscular dystrophy of dogs. *Nature*, **334**, 154–156.
39. Gyurko, R., Leupen, S. and Huang, P.L. (2002) Deletion of exon 6 of the neuronal nitric oxide synthase gene in mice results in hypogonadism and infertility. *Endocrinology*, **143**, 2767–2774.
40. Petrof, B.J., Shrager, J.B., Stedman, H.H., Kelly, A.M. and Sweeney, H.L. (1993) Dystrophin protects the sarcolemma from stresses developed during muscle contraction. *Proc. Natl Acad. Sci. U.S.A.*, **90**, 3710–3714.
41. Brooks, S.V. (1998) Rapid recovery following contraction-induced injury to in situ skeletal muscles in mdx mice. *J. Muscle Res. Cell Motil.*, **19**, 179–187.
42. Dellorusso, C., Crawford, R.W., Chamberlain, J.S. and Brooks, S.V. (2001) Tibialis anterior muscles in mdx mice are highly susceptible to contraction-induced injury. *J. Muscle Res. Cell Motil.*, **22**, 467–475.
43. Martinez-Ruiz, A., Araujo, I.M., Izquierdo-Alvarez, A., Hernansanz-Agustin, P., Lamas, S. and Serrador, J.M. (2013) Specificity in S-nitrosylation: a short-range mechanism for NO signaling?. *Antioxid. Redox Signal.*, **19**, 1220–1235.
44. Lima, B., Forrester, M.T., Hess, D.T. and Stamler, J.S. (2010) S-nitrosylation in cardiovascular signaling. *Circ. Res.*, **106**, 633–646.
45. Percival, J.M., Anderson, K.N., Gregorevic, P., Chamberlain, J.S. and Froehner, S.C. (2008) Functional deficits in nNOSmu-deficient skeletal muscle: myopathy in nNOS knockout mice. *PloS One*, **3**, e3387.
46. Chen, Y.W., Nagaraju, K., Bakay, M., McIntyre, O., Rawat, R., Shi, R. and Hoffman, E.P. (2005) Early onset of inflammation and later involvement of TGFbeta in Duchenne muscular dystrophy. *Neurology*, **65**, 826–834.
47. Chen, Y.W., Zhao, P., Borup, R. and Hoffman, E.P. (2000) Expression profiling in the muscular dystrophies: identification of novel aspects of molecular pathophysiology. *J. Cell Biol.*, **151**, 1321–1336.
48. Porter, J.D., Khanna, S., Kaminski, H.J., Rao, J.S., Merriam, A.P., Richmonds, C.R., Leahy, P., Li, J., Guo, W. and Andrade, F.H. (2002) A chronic inflammatory response dominates the skeletal muscle molecular signature in dystrophin-deficient mdx mice. *Hum. Mol. Genet.*, **11**, 263–272.
49. Sharma, K.R., Mynhier, M.A. and Miller, R.G. (1995) Muscular fatigue in Duchenne muscular dystrophy. *Neurology*, **45**, 306–310.
50. Angelini, C. and Tasca, E. (2012) Fatigue in muscular dystrophies. *Neuromuscul. Disord.*, **22**, S214–e220.
51. Gregorevic, P., Plant, D.R., Leeding, K.S., Bach, L.A. and Lynch, G.S. (2002) Improved contractile function of the mdx dystrophic mouse diaphragm muscle after insulin-like growth factor-I administration. *Am. J. Pathol.*, **161**, 2263–2272.
52. Gregorevic, P., Plant, D.R. and Lynch, G.S. (2004) Administration of insulin-like growth factor-I improves fatigue resistance of skeletal muscles from dystrophic mdx mice. *Muscle Nerve*, **30**, 295–304.
53. Allen, D.G., Lamb, G.D. and Westerblad, H. (2008) Skeletal muscle fatigue: cellular mechanisms. *Physiol. Rev.*, **88**, 287–332.
54. Jaffrey, S.R., Erdjument-Bromage, H., Ferris, C.D., Tempst, P. and Snyder, S.H. (2001) Protein *S*-nitrosylation: a physiological signal for neuronal nitric oxide. *Nat. Cell Biol.*, **3**, 193–197.
55. Landino, L.M., Koumas, M.T., Mason, C.E. and Alston, J.A. (2007) Modification of tubulin cysteines by nitric oxide and nitroxyl donors alters tubulin polymerization activity. *Chem. Res. Toxicol.*, **20**, 1693–1700.
56. Belanto, J.J., Mader, T.L., Eckhoff, M.D., Strandjord, D.M., Banks, G.B., Gardner, M.K., Lowe, D.A. and Ervasti, J.M. (2014) Microtubule binding distinguishes dystrophin from utrophin. *Proc. Natl Acad. Sci. U.S.A.*, **111**, 5723–5728.
57. Selemidis, S., Dusting, G.J., Peshavariya, H., Kemp-Harper, B.K. and Drummond, G.R. (2007) Nitric oxide suppresses NADPH oxidase-dependent superoxide production by *S*-nitrosylation in human endothelial cells. *Cardiovasc. Res.*, **75**, 349–358.
58. Shkryl, V.M., Martins, A.S., Ullrich, N.D., Nowycky, M.C., Niggli, E. and Shirokova, N. (2009) Reciprocal amplification of ROS and Ca(2+) signals in stressed mdx dystrophic skeletal muscle fibers. *Pflugers Arch.*, **458**, 915–928.
59. Whitehead, N.P., Yeung, E.W., Froehner, S.C. and Allen, D.G. (2010) Skeletal muscle NADPH oxidase is increased and triggers stretch-induced damage in the mdx mouse. *PloS One*, **5**, e15354.
60. Khairallah, R.J., Shi, G., Sbrana, F., Prosser, B.L., Borroto, C., Mazaitis, M.J., Hoffman, E.P., Mahurkar, A., Sachs, F., Sun, Y. *et al.* (2012)

Microtubules underlie dysfunction in Duchenne muscular dystrophy. *Sci. Signal.*, **5**, ra56.
61. Millay, D.P., Goonasekera, S.A., Sargent, M.A., Maillet, M., Aronow, B.J. and Molkentin, J.D. (2009) Calcium influx is sufficient to induce muscular dystrophy through a TRPC-dependent mechanism. *Proc. Natl Acad. Sci. U.S.A.*, **106**, 19023–19028.
62. Bulfield, G., Siller, W.G., Wight, P.A. and Moore, K.J. (1984) X chromosome-linked muscular dystrophy (mdx) in the mouse. *Proc. Natl Acad. Sci. U.S.A.*, **81**, 1189–1192.
63. Schneider, C.A., Rasband, W.S. and Eliceiri, K.W. (2012) NIH Image to ImageJ: 25 years of image analysis. *Nat. Methods*, **9**, 671–675.
64. Briguet, A., Courdier-Fruh, I., Foster, M., Meier, T. and Magyar, J.P. (2004) Histological parameters for the quantitative assessment of muscular dystrophy in the mdx-mouse. *Neuromuscul. Disord.*, **14**, 675–682.
65. Gottfried, E., Kunz-Schughart, L.A., Weber, A., Rehli, M., Peuker, A., Muller, A., Kastenberger, M., Brockhoff, G., Andreesen, R. and Kreutz, M. (2008) Expression of CD68 in non-myeloid cell types. *Scand. J. Immunol.*, **67**, 453–463.